AST 300B – Spring 2018

In-class/take-home Problems Due: Wednesday Feb. 7

15. Optical forbidden line ratios in HII regions may be used to derive the temperature and density. The graph below shows how the OIII (doubly ionized oxygen) line ratio of 4364/5008 (Angstroms) depends on T. This line ratio is measured in a spectrum toward an HII region to be I(4364)/I(5008) = 0.003. The reddening due to dust between these two wavelengths is measured to be A(4363) – A(5008) = 0.76 mag. Estimate the T of this HII region if $n \sim 10^3$ cm^{-3}.

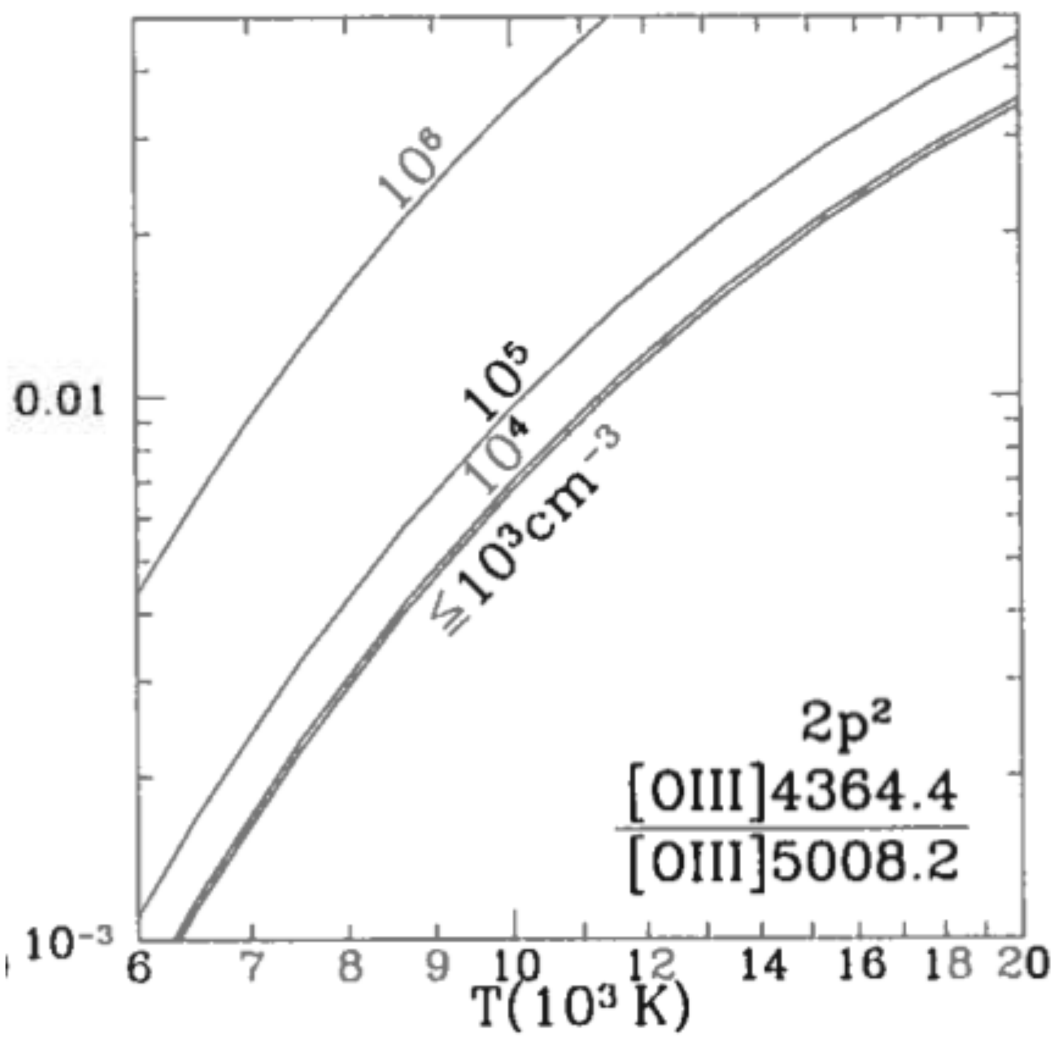

FIGURE 1: Plot of the intensity ratio of 4364/5008 for OIII vs. electron thermal temperature in HII regions. The different curves correspond to different electron number densities (cm^{-3}).

16. Dust grains can coagulate and grow in size in dense environments. Furthermore, in cold environments, ices can form on the surface of the grains. Both of these effects change the opacity of the grains. In a classic paper by Ossenkopf & Henning (1994 A&A, 291, 943), the dust opacities were calculated for dust grains that have coagulated at different densities and with different amounts of H_2O ice. Column 5 for grains coagulated at a density of 10^6 cm^{-3} with thin ice mantles (called "OH5" dust) is a very popular model used to approximate the opacities of dust in star forming regions. Assume the dust opacity at $\lambda >= 350$ μm is well described by a single power law with $\kappa_\nu \sim \lambda^{-\beta}$. Calculate β for OH5 dust.

V. Ossenkopf & Th. Henning: Dust opacities for protostellar cores

Table 1. (continued)

Initial distribution:		MRN			MRN with thin ice mantles			MRN with thick ice mantles	
Gas density [cm^{-3}]	–	10^6	10^8	–	10^6	10^8	–	10^6	10^8
	Fig. 1a	Fig. 2a	Fig. 2b	Fig. 1b	Fig. 3a	Fig. 3b	Fig. 1c	Fig. 4a	Fig. 4b
λ [μm]					κ [cm^2/g]				
5.41e+1	9.05e+1	1.45e+2	2.19e+2	1.92e+2	2.80e+2	3.48e+2	9.79e+2	1.19e+3	1.34e+3
6.31e+1	7.16e+1	1.16e+2	1.76e+2	1.43e+2	2.11e+2	2.63e+2	6.59e+2	8.21e+2	9.37e+2
7.36e+1	5.60e+1	9.19e+1	1.41e+2	1.05e+2	1.58e+2	1.97e+2	4.25e+2	5.41e+2	6.22e+2
8.58e+1	4.37e+1	7.32e+1	1.14e+2	7.76e+1	1.18e+2	1.47e+2	2.62e+2	3.40e+2	3.90e+2
1.00e+2	3.44e+1	5.92e+1	9.38e+1	5.56e+1	8.65e+1	1.07e+2	1.27e+2	1.72e+2	1.95e+2
1.17e+2	2.70e+1	4.82e+1	7.86e+1	4.30e+1	6.75e+1	8.30e+1	8.30e+1	1.13e+2	1.28e+2
1.36e+2	2.07e+1	3.88e+1	6.57e+1	3.30e+1	5.25e+1	6.45e+1	5.73e+1	7.91e+1	8.85e+1
1.58e+2	1.59e+1	3.16e+1	5.61e+1	2.53e+1	4.09e+1	5.03e+1	3.98e+1	5.57e+1	6.19e+1
1.85e+2	1.17e+1	2.53e+1	4.74e+1	1.87e+1	3.07e+1	3.77e+1	2.71e+1	3.84e+1	4.23e+1
2.26e+2	8.16e+0	1.95e+1	3.89e+1	1.30e+1	2.17e+1	2.67e+1	1.75e+1	2.51e+1	2.74e+1
3.50e+2	3.64e+0	1.13e+1	2.58e+1	5.91e+0	1.01e+1	1.24e+1	7.79e+0	1.12e+1	1.20e+1
5.00e+2	1.77e+0	7.61e+0	1.98e+1	2.90e+0	5.04e+0	6.21e+0	3.79e+0	5.50e+0	5.72e+0
7.00e+2	9.09e−1	4.56e+0	1.25e+1	1.48e+0	2.57e+0	3.18e+0	1.93e+0	2.81e+0	2.93e+0
1.00e+3	4.77e−1	2.74e+0	7.85e+0	7.81e−1	1.37e+0	1.69e+0	1.01e+0	1.48e+0	1.54e+0
1.30e+3	3.09e−1	1.99e+0	5.86e+0	5.11e−1	8.99e−1	1.11e+0	6.48e−1	9.62e−1	1.00e+0

FIGURE 2: Portion of Table 1 from Ossenkopf & Henning 1994 (p. 949).